ISTANBUL TECHNICAL UNIVERSITY ★ GRADUATE SCHOOL OF SCIENCE ENGINEERING AND TECHNOLOGY

TUG T60 OPTICAL AND SWIFT X-RAY ARCHIVAL OBSERVATIONS OF TRANSITIONAL MILLISECOND PULSAR PSR J1023+0038

M.Sc. THESIS

Hesaum FARAZI MAJD

Department of Physics Engineering

Physics Engineering Programme

SEPTEMBER 2017

ISTANBUL TECHNICAL UNIVERSITY ★ GRADUATE SCHOOL OF SCIENCE ENGINEERING AND TECHNOLOGY

TUG T60 OPTICAL AND SWIFT X-RAY ARCHIVAL OBSERVATIONS OF TRANSITIONAL MILLISECOND PULSAR PSR J1023+0038

M.Sc. THESIS

Hesaum FARAZI MAJD
(509131120)

Department of Physics Engineering

Physics Engineering Programme

Thesis Advisor: Prof. Dr. Kazım Yavuz Ekşi

SEPTEMBER 2017

İSTANBUL TEKNİK ÜNİVERSİTESİ ★ FEN BİLİMLERİ ENSTİTÜSÜ

GEÇİŞLİ MİLİSANİYE PULSARI PSR J1023+0038'in TUG T60 OPTİK VE SWİFT X-IŞINI ARŞİV GÖZLEMLERİ

YÜKSEK LİSANS TEZİ

Hesaum FARAZI MAJD
(509131120)

Fizik Mühendisliği Anabilim Dalı

Fizik Mühendisliği Programı

Tez Danışmanı: Prof. Dr. Kazım Yavuz Ekşi

EYLÜl 2017

Hesaum FARAZI MAJD, a M.Sc. student of ITU Graduate School of Science Engineering and Technology 509131120 successfully defended the thesis entitled " TUG T60 OPTICAL AND SWIFT X-RAY ARCHIVAL OBSERVATIONS OF TRANSITIONAL MILLISECOND PULSAR PSR J1023+0038 ", which he prepared after fulfilling the requirements specified in the associated legislations, before the jury whose signatures are below.

Thesis Advisor :	**Prof. Dr. Kazım Yavuz Ekşi** Istanbul Technical University	.....
Jury Members :	**Doç . Dr. Tolga Güver** Istanbul University	.....
	Doç . Dr. Savaş Arapoğlu Istanbul Technical University	.....
		.....

Date of Submission : **05 September 2017**
Date of Defense : **05 September 2017**

To my family,

FOREWORD

I would like to express my gratitude to my supervisor Prof. Kazım Yavuz Ekşi who gave me the chance of entering the glorious world of neutron stars. Beyond the science he taught me, he is a great example of a diligent man.
I would like to express my sincere thanks to my co-advisor Assoc. Prof. Dr. Tolga Güver for teaching me observational techniques I used in the thesis.
I am obliged to thanks, Turkish National Observatory (TUG) for providing the optical data of this work through their T60 telescope.
I am grateful to Dr. Can Güngör for his endless help through my data analysis and postdoc Sinem Şaşmaz who taught me X-ray analysis and help me to finish the thesis.
Thanks to my dear friends in Istanbul Technical universities High Energy Astrophysics Laboratory, İbrahim Ceyhun Andaç and Sercan Çıkıntoğlu for their help in my programming problem.
I would like to thanks to my dear friends that help me to feel at home in a foreign country, Begüm İnal Turna, Hacire Uğur, İlknur Köseoğlu, Oğuz Gürcüoğlu, Onur Karayalçın and Sare Akgöz.
Finally, I would like to thanks my mother, Hakimeh Moghimi Oskouyi, my brother Soheil Farazi Majd, my love Simin Timar for their enormous supports and my father, my inimitable life supporter that has passed away, ADEL FARAZI MAJD.

September 2017

Hesaum FARAZI MAJD
B.Sc.

TABLE OF CONTENTS

Page

ABBREVIATIONS

Å : Angstrom
App : Appendix
CCD : Charge Coupled Device
CCO : Central Compact Object
CV : Cataclysmic Variable
EM : Electromagnetic
FBQS : First Bright Quasar Survey
HMXB : High Mass X-ray Binary
INS : Isolated Neutron Star
IRAF : Image Reduction and Analysis Facility
IMXB : Intermediate Mass X-ray Binary
keV : Kilo Electron Volt
LMXB : Low Mass X-ray Binary
MSP : Millisecond Pulsar
RPP : Rotation Powered Pulsar
TMP : Transitional Millisecond Pulsar
TUG : Turkish National Observatory

LIST OF TABLES

Page

LIST OF FIGURES

Page

TUG T60 OPTICAL AND SWIFT X-RAY ARCHIVAL OBSERVATIONS OF TRANSITIONAL MILLISECOND PULSAR PSR J1023+0038

SUMMARY

After the discovery of the fast rotating millisecond pulsars (MPS), it was suggested that these sources (are produced) by accretion of matter onto neutron stars in low mass X-ray binary (LMXB) systems. Accretion of matter imposes angular momentum to the neutron star and spins it up to periods of milliseconds. Discoveries of accreting millisecond X-ray pulsars (AMXPs) and transitional millisecond pulsars (TMP) illustrated the expected link between MPSs and LMXBs.
PSR J1023+0038 is the first observed TMP that not only experiences both MPS and LMXB phases but also changed its state two times .
We performed optical and X-ray observations of this source between 2015/01/01 and 2015/04/30 to investigate any other phase change and define correlation in luminosity between these two bands in different phases.
Optical data were collected through TUG T60 telescoped and UBVRI filter. We used 74 data frames with 60 second exposure time in R band for optical analysis. Optical data reduction was done through `iraf` program and differential photometry method was used by use of 5 comparison star nearby the main source in data frames.
Swift XRT telescope archival data for same time interval with optical observations was selected for further analysis. At all 20 swift observation was available for the desired time interval. X-ray data analysis and fitting were done through the `HEASOFT` program. We fit the data with absorbed powerlaw model with n_h parameter fixed.
From optical observation, we reach to the mean optical luminosity of 16.31 that is shown no significant change in optical luminosity of the system.
X-ray analysis leads to a mean 0.3-10 keV luminosity of 2.63×10^{33} erg/s that illustrate the system shows no phase change during the observation interval.
According to lack of simultaneous observations in two band, we can not define any X-ray/optical correlation.

GEÇİŞLİ MİLİSANİYE PULSARI PSR J1023+0038'in TUG T60 OPTİK VE SWİFT X-IŞINI ARŞİV GÖZLEMLERİ

ÖZET

Nötron yıldızları supernova patlamalarında doğarlar. Büyük kütleli yıldızlar (>14 Güneş kütlesi) evrimlerinin son aşamasında çekirdeklerine doğru çökerlre ve yıldızın diğer katmanları püskürtülür. Geride kalan tıkız çekirdek $\sim$1.4 $M\odot$ ve $\sim$10 km yariçapına sahip olan bir nötron yıldızını oluşturur.

Nötron yıldızlarının alt kategorisinde rotation powered pulsarlar, accreting power pulsarlar, magnetarlar, central compact objectler ve izole notron yıldızları yer alırlar.

Accretion powered pulsarlarda nötron yıldızının üzerine aktarılan maddenin kütle çekimsel enerjisi ışımaya sebep olurken rotation powered pulsarlarda dönme hızınının azalmasıış ımaya neden olur.

Düşük kütleli X-ışın ciftleri ve büyük kütleli X-ışın çiftleri accretining powered pulsar kategorisinin altında yer alırlar. Düşük kütleli X-ışın çiftleri bir nötron yıldızıve bir Güneş kutlesinden düşük kütleye sahip olan yaşlı yıldızlardan oluşur. Bu nesnelerde nötron yıldıd ız nın çevresinde bir disk oluşur ve madde yüksek oranda Roche lobe taşması (Roche lobe overflow) yoluyla diskten nötron yıldının üzerine aktarılmaktadır. Nötron yıldızının üzerine aktarılan madde, diskin iç yariçapından ayrılıp, nötron yıldının manyetik alan çizgilerini takip ederek nötron yıldızının kutuplarina duşerler. Nötron yıldının dönme ve manyetik ekseni aynı doğrultuda olmadığından dolayı kutuplardan gelen ışımayıatma (puls) şeklinde gözlemleriz.

İlk Rotation Powered pulsar 1967'de Jocelyn Bell ve Anthony Hewish tarafından keşfedildi. Milisaniye pulsarları bu kategorinin icinde yer alırlar. İlk milisaniye pulsarı 1975 yılında keşfedildi. Bu nesneler yüksek dönme hızına sahiptirler ve aynı zamanda düşük manyetik alanları onların isole radyo pulsarlara göre daha yaşli olduklarını gösteriyor. 1982 yılında Ali Alpar ve Radhakrishnan tarafından önerilen senaryoda milisaniye pulsarları ve düşük kütleli X-ışın ciftlerinin arasında bir bağ olduğu iddia edildi. Bu senaryoya göre, düşük kütleli X-ısın ciftlerinnde, aktarılan madde açısal momentuma sahip oldğu için ve bu hızı zaman zaman sistemde olan nötron yıldızına aktardığı icin, nötron yıldızıyüksek bir dönme hızına sahip olabilir. Ayrıca uzun süre madde aktarımından dolayi yıldız manyetik alan gücünü zamanla kaybeder.

1974 ve 1982'de keşfedilen accreting milisaniye X-ışın pulsarı ve transitional milisaniye Pulsar'lr bu senaryoyu doğrulamaktadır.

Transitional milisaniye pulsar sistemleri, bazen düşük kütleli X-ış ın çiftleri fazında olup, bir süre sonra milisaniye radyo pulsarı fazına geçis yaparlar ve geçis yaptıktan sonra radyo-optik-X-ışın ve hatta Gamma ışınlarında önemli değişikler gösterirler. Bu sistemlerin farklı yönlerde incelenmesi milisaniye pulsarları ve düşük kütleliX-ış ın çiftlerinin arasında olan bağı ve onların evrimlerini anlamıza yardımcı olabilirler. PSR J1023+0038, ilk keşfedilen geçişli milisaniye pulsarıdır.

Bu çalışmada PSR J1023+0038 kayanağının , optik ve X-ış ınida gözlemleyerek, hangi

fazda olduğnu ve optik ve X-ış ını parlaklıklarnın arasındaki korelasyonu belirlemeye çalıstık. PSR J1023+0038, 2000 yılında Bond tarafından keşfedildi. Bu kaynağın 2000 yılındaki gözlemleri çevresinde bir disk olduğunu gösteriyordu. 2000-2008 aralığında kaynak dü şük kutleli X-ış ın cıftleri özellikerine sahipti yalnız 2008 de kaynak optik ve X-ışınında değişiklikler göstermeye başladı ve radyo ışıması yaymaya başladı. Bu süreç 2013 yılına kadar sürdü ve tekrar 2013 yılında sistem dü şük kutleli X-ış ın cıftleri fazına geçti. 2013'den bu yana sistem dü şük kutleli X-ışın cıft fazında devam etmmektdir. PSR J1023+0038 sisteminin özellikleri :

- Orbital Period: 4.75 hour
- Pulse Period: 1.69 ms
- NS Mass: $\sim 1.4 M_{\odot}$
- Donor Mass: $\sim 0.2 M_{\odot}$
- B (Magnetic field): 10^8 G
- L_X in MPS state: $\sim 10^{32}$ erg/s
- L_X in LMXB state: $\sim 10^{33-35}$ erg/s
- Distance: ~ 1.37 *rmkpc*

Optik verilri 2015 Şubat - Nisan aylar arasında Türkiye Ulusal Gözlemevi (TUG) T60 teleskopuyla, "Galaktik Süreksiz Düşük Kütleli X-ışın Cıftlerinin Herhangi bir Dalgaboyunda Tespit edilecek Patlamalarının Takip Gözlemleri" projesi kapsamında ve UBVRI filtresini kullanılarak gözlemlenmiştir. Kötü hava koşullari nedeniyle optik analizlerde sadece R bandında olan gözlemler seçildi ve kaynağ ın R bandinda daha parlak olmasi, eşlikçinin G yıldızları kategorisinden olduğnu gosteriyor. 224 gozlemden yalnız 74 gozlem, 60 saniyelik poz süresiyle analiz için uygun göründü. veri kalibrasiyon aşamasında Dark, Flat ve Bias düzeltmeleri `IRAF` programı kullanılarak yapılmıştır. Daha doğru bir parlaklik ölçmek icin, 5 örnek yildiz secerek, fark fotometri yöntemi uygulanmiştır.
X-ışınında analiz yapmak için aynı tarih arasında (2015 Subat - Nisan) Swift XRT teleskop gözlem arşivini kullandık. `Heasoft v. 6.19` paketleri X-ışın gözlem analiz ve modelleme için kullanıldı. Her bir gözlem için kaynak ve arkaplan alanları40 yay saniyesi yarıçapında çembersel şekilde seçildi, kaynak ve arkaplan tayflarıelde edildi. X-ışını tayfları `absorbed powerlaw` modeliyle fit edildi ve foton indeksi ortalaması, $\Gamma \simeq 1.6$ elde edildi. Modelleme sürecinde tüm gozlemler için N_H degeri $3.8 \times 10^{20} \mathrm{cm}^{-2}$ sabitlendi.
PSR J1023+0038 kaynagının optik parlaklığını 15.57 ve 16.95 aralığında bulduk. Optik parlaklığının ~ 1.38 değismesi sistemin yörünge donuşumunden kaynaklana bilmektedir, yanlız bunu kesin söyleyebilmek için daha yuksek zaman çözünürlüğünde veriye ithiyaç duyulmaktadır.
X-ışın analizinden çikan sonuçlara göre, X-ışın parlaklığı1.4×10^{33}ve4.9×10^{33} aralığında olduğunu belirledik. Bu parlaklığa göre sistemin halen düşük X-ışın fazında olduğunu ve diskten nötron yıldızının üzerine madde aktarımı olmadığını söyliyebiliriz. Her iki bantta aynı zamanlarada alınmış yeterli sayıda gözlem olmadığı için X-ışın/optik korelasyonu incelenmedı ve

hakkıında neyazık kı yorum yapamıyoruz.

1. INTRODUCTION

1.1 Neutron stars

Neutron stars are remnants of high mass stars, compact objects with radius around 10 kilometers and mass around 1.4 $M_{\odot}$. These parameters correspond to a density of $\rho \sim 10^{14}$ gr/cm^3 (10^{14} times denser than the Earth). As a massive star ($M \sim 15\ M_{\odot}$) consumes its source for the fusion reactions it acquires an iron core. Subsequently the iron core collapses to a small radius and releases gravitational energy which powers the supernova. For the collapsed core the gravitational force is balanced by the electron and neutron degeneracy pressures and the core gets stable. Since the angular momentum and magnetic flux of the star should be conserved after the explosion, neutron stars possess inordinate high spin and magnetic field.

Different types of neutron stars are categorized by the source powering their emission. Rotation-powered pulsars (RPP) (powered by spindown), magnetars (released by decaying magnetic field), isolated neutron stars (INS) and central compact objects (CCO) (powered by latent heat of the neutron star matter), accretion-powered neutron stars (gravitational energy released by accretion) are some of these classes.

1.2 Rotation powered pulsars

Pulsars were discovered in 1967 by Jocelyn Bell and Anthony Hewish. In the pulsar discovery paper [1] they related the radio pulsations to oscillations of compact stars but later it was suggested by Gold [2] that rotation of the compact star leads to the pulsation behavior. The inclination angle between the rotation and magnetic axis of the neutron star causes the lighthouse effect which leads to the observation of pulses (Figure 1.1).

In this type of pulsars, the main source of emission is the energy released by spin down. This energy is propagated in a wide range of wavelengths from radio to gamma rays. Up to now more than 2000 RPPs are discovered. The RPPs have rotation periods

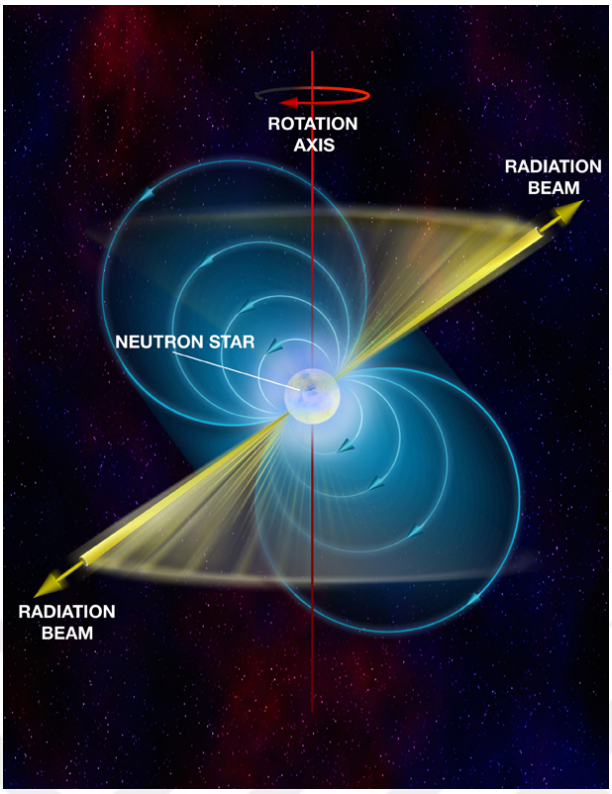

Figure 1.1 : Standard model of rotational pulsars [3]

between milliseconds to several seconds [4] and are divided into two main groups, normal pulsars with characteristic ages $\tau < 100$ Myr, and millisecond pulsars (MSP) with $\tau \gtrsim 100$ Myr. Indeed, it is believed that neutron stars in low mass X-ray binaries are the progenitors of MPSs. MPSs spin up by accretion from their companion in a binary system for about a billion years [5].

1.3 Accretion powered pulsars

The second type of pulsars are accretion-powered pulsars that most of the dispersed energy originates from the gravitational potential of the matter that accrete onto the surface of the neutron star and the released energy is mostly detected in the X-ray band. Accretion-powered pulsars live in binary systems and gasous matter from the companion reach the surface of the neutron star either by steller wind or a disk. Luminosity generated by accretion of gas is [6]:

$$L_X = \frac{GM\dot{M}}{R} \approx 1.3 \times 10^{37} \dot{M}_{17} \left(\frac{M}{M_\odot}\right) R_6^{-1} \text{ erg s}^{-1}. \quad \textbf{(1.1)}$$

Here G, M, R and $\dot{M}$ refer to the gravitational constant, mass of the neutron star, radius of the NS and the rate of mass accretion, respectively ($R_6 = \frac{R}{10^6}\ cm$, $\dot{M}_{17} = \frac{\dot{M}}{10^{17}}\ g\ s^{-1}$) . For an X-ray source with $L_X \sim 10^{37}$ erg s^{-1} accretion rate is 10^{17} g s^{-1}.

Intense magnetic fields of neutron stars steer the gas particles toward the magnetic poles of the star through a flux-frozen flow [7, 8]. The region that particles follow the magnetic field lines around the star is called the magnetosphere of the neutron star.

Accretion-powered pulsars can be classified into three groups according to the mass of the companion star as high mass X-ray binaries (HMXBs), intermediate mass X-ray binaries (IMXBs), low mass X-ray binaries (LMXBs). In all three types there is a common situation, the companion fills or very nearly fills its Roche lobe.

HMXBs consist of a neutron star and an O/B or Be-type star as a companion. These systems normally survive less than LMXBs due to fast evolution of their massive companion. Accretion by strong stellar wind from O/B supergiant companion feeds the neutron star and leads to bright X-ray emission. This phase lasts about $10^4 - 10^5$ years and near the end of this time Roche lobe overflow process also starts. In HMXBs with Be-type star companion, since the primordial binary has less mass, the orbits of these systems are wider and the companion lies deep inside its Roche lobe.

There are two classifications with very similar specifications in low mass X-ray binaries, cataclysmic variables (CVs) and low mass X-ray binaries (LMXBs). The main difference is that in CVs compact object is a white dwarf, on the other hand, LMXBs posses a neutron star. In general, LMXBs are born through one of these two scenarios, the progenitor has a much more mass ($M_{progenitor} \gtrsim 12 M_\odot$) than the progenitor in CVs, or accretion onto the white dwarf in CVs augments the mass above the Chandrasekhar mass and the white dwarf collapses into a neutron star and LMXB is born [9] (accretion-induced collapse). In the following we will discuss some properties of LMXB systems. One of the important properties is the orbital period (binary period) of these systems. As it is shown below, the orbital period just depends on the average density of the donor [10]

$$P = 8.9 \left(\frac{M_2}{M_\odot}\right)^{-\frac{1}{2}} \left(\frac{R_2}{R_\odot}\right)^{\frac{3}{2}} \text{ hr} = 8.9 \left(\frac{\rho_2}{\rho_\odot}\right)^{-\frac{1}{2}} \text{ hr} . \qquad \textbf{(1.2)}$$

The characteristic relation between the orbital period and donors mass have been made by using this equation and mass-radius relation for possible companions of these systems. Table 1.1 illustrates the mass-radius and mass-orbital period relations for donors of these systems [10].

Table 1.1 : Mass-radius and mass-orbital period relations for donors of LMXBs systems [10].

Companion Type	$M_2 - R_2$ Relation	$M_2 - P$ Relation
Main Sequence	$R_2/R_\odot \approx M_2/M_\odot$	$P \approx 8.9(M_2/M_\odot)$ hr
He Main Sequence	$R_2/R_\odot \approx 0.2M_2/M_\odot$	$P \approx 0.89(M_2/M_\odot)$ hr
White Dwarf	$R_2/R_\odot \approx 0.0115(M_2/M_\odot)^{1/3}$	$P \approx 40(M_\odot/M_2)$ sec

These data are very practical for estimating the orbital periods or masses of the companion stars.

There are exceptions that do not belong to any of the above categories, IMXBs. A neutron star and a 2.5 $M_\odot$ companion is the general structure of an **IMXB**. These systems have very eccentric orbits and after about 10^7 y, their orbital periods ascend from $\sim$ 5.7 d to $\sim$ 1.7 d [11]. Moreover, in the supernova a kick is imposed to them and they run away with $v \sim 140$ km s^{-1}. Accretion in IMXBs proceeds via Roche lobe overflow. The source Her X-1 is an example of these systems.

1.4 Recycling Scenario

The scenario of the formation of the radio pulsars needed to be renewed by the discovery of the PSR 1913+16 [12], in 1974, that belongs to a close binary system . It was believed that isolated radio pulsars were formed by disruption of the close binary systems after the supernova explosion. According to the understanding of neutron stars in 70's, the short rotation period of the PSR 1913+16 could be explained by the young age of the pulsar but on the under hand young pulsars like Crab and Vela possessed high magnetic fields that that was not true for the magnetic field of PSR 1913+16. Before the discovery of PSR 1913+16 it was suggested by Bisnovatyi-Kogan [13] that magnetic fields of the neutron stars in binary system could decay through the accretion process and the system could possess a weak magnetic field after accretion stops. It was proposed by Bisnovatyi-Kogan that PSR 1913+16 passed through the accretion phase and spun up while its magnetic field decreased through the accretion

process [14]. After the explosion of its companion, X-ray pulsar entered the radio pulsar phase.

Another fast rotating pulsar with inordinate characteristics was discovered by Backer at 1982 [15]. The source 4C21.53 had the fast spin period and low magnetic field with no supernova remnant around it. Later it was suggested by Alpar that the source 4C21.53 and the other similar pulsars belong to a new class of radio pulsars, millisecond pulsars [5] which originate in close binary systems with X-ray pulsars as progenitors. Similarities to PSR 1913+16 characteristics reinforces the idea that millisecond pulsars are 'recycled'. Recycling scenario propose that radio pulsars with millisecond rotation periods are spun up during the long time accretion from a Keplerian disk in low mass X-ray binary systems while their magnetic fields decay in this process [5, 13, 16].

New discoveries through the time enhanced the validity of the recycling scenario. The first one was the discovery of the first Accreting Millisecond X-ray Pulsar (AMXP), SAX J1808.4-3658, in 1998 [17]. Discovery of the transitional millisecond pulsars was another strong proof of recycling scenario and ascertained the link between LMXBs and MPs. Many investigations have begun after the discovery of TMPs to study the different aspects of these sources and resolving the dark side of the MPs evolution.

1.5 Transitional Millisecond Pulsars (TMPs)

TMPs are uniqe systems that transit between low mass X-ray binaries and millisecond radio pulsars. Indeed, in some period of time they emit in the radio band and possess millisecond pulsar properties. At a later time the radio emission vanishes and the objects begin to show X-ray emission. Up to now three TMPs (and a fourth candidate) are discovered.

- J1023+0038
- XSS J12270-4859
- M28I
- 1RXS J154439.4-112820

X-ray observations of these objects show three different stages for the X-ray luminosity, radio pulsar stage with $L_X \sim 10^{32}$ erg/sec, intermediate X-ray stage with

$L_X \sim 10^{33} - 10^{34}$ erg/sec and outburst stage with $L_X \sim 10^{36}$ erg/sec. Through this work we try to study different aspects of PSR J1023+0038 ,the first discovered source of TMPs category, in optical and X-ray wavelength and exploit correlation between optical and X-ray observation and specifying the system phase as LMXB or MP. Table 1.2 shows the characteristics of the PSR 1023+0038 binary system.

Table 1.2 : PSR J1023+0038.

PSR J1023+0038	
Orbital Period	4.75 hour
Pulse Period	1.69 ms
NS Mass	$\sim 1.4 M_\odot$
Donor Mass	$\sim 0.2 M_\odot$
B (Magnetic field)	10^8 G
L_X in MPS state	$\sim 10^{32}$ erg/s
L_X in LMXB state	$\sim 10^{33-35}$ erg/s

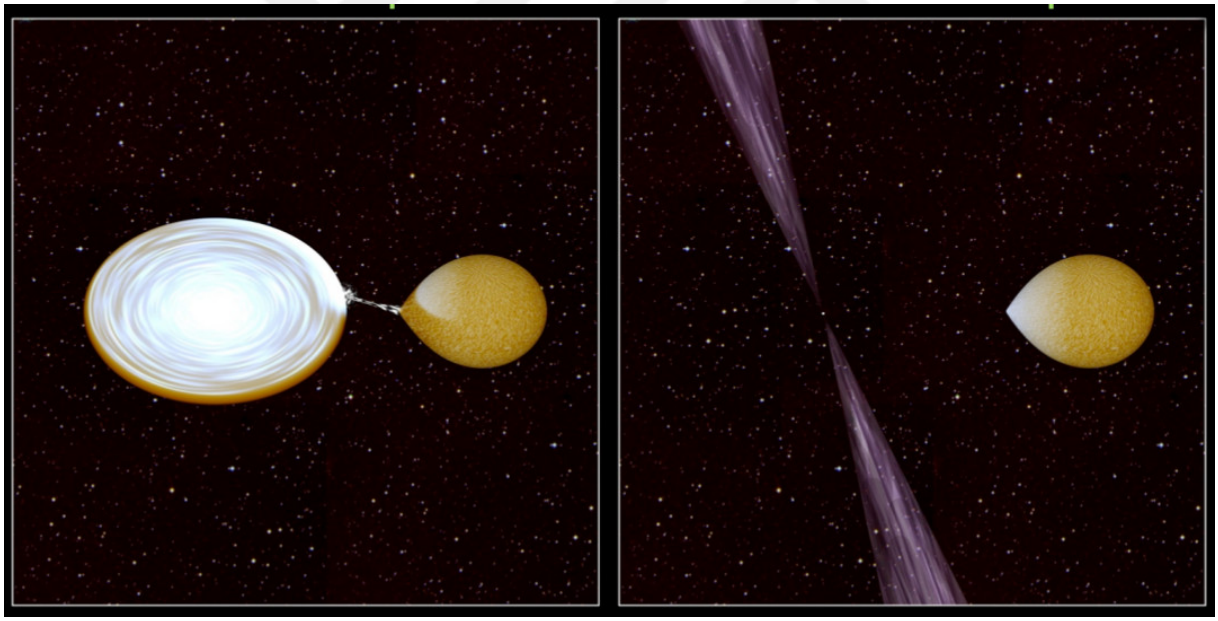

Figure 1.2 : Schematic of TMPs in two different phase. Left: LMXB phase with accretion disk around the neutron star. Right: MSP phase with radio beams from the poles of the neutron star and no accretion from the donor.

2. GENERAL PROPERTIES OF PSR J1023+0038

2.1 Observations of PSR J1023+0038

PSR J1023+0038 was first source that has been categorized as CV due to radio observation [18] through the FIRST (The Faint Image of the Radio Sky at Twenty Centimeters) Bright Quasar Survey (FBQS) [19–21] and following optical observation seemed to confirm the case [18]. Candidates of the FBQS were FIRST radio sources that have optical counterpart in the APM (Automatic Plate Measuring) catalog. A radio source among the FBQS candidates was idetifined as a Galactic star with uncommon spectrum. It was inferred that it is a previously unknown CV. 1".6 away from the coordination of the source, there was a faint stellar object according to the APM catalog.

The spectrum that was obtained at 2000 May 6 with Lick Observatory 3 m telescope was dominated by a blue continuum with superposed emission lines of the Balmer series: He I, and He II [18]. This spectrum was similar to the spectrum of the cataclysmic variables in quiescence. Stronger lines of the He I and He II in comparison with dwarf novae offered that the source can be classified as the magnetic or AM Herculis type CVs [18]. Exploring the archived data of the Sloan Digital Sky Survey (SDSS), both astrometry and photometry data, illustrated that the spectrum was similar to that obtained from Lick Observatory [18]. In addition, in SDSS spectrum the emission lines were resolved into double-peaked profiles and it was suggested that the system might harbour an accretion disk implying that the source can be a DQ-Herculis type magnetic CV [18]. Since CVs show rapid optical variations, further photometric observations were done to investigate these variations of PSR J1023+0038. Further observations in 2000 November and December recorded variation in PSR J1023+0038 light curve, and this variation affirmed that the source could be categorized as a CV at that time [18].

The source was observed for different purposes (spectroscopy, filter photometry, I (infrared) Time-series Photometry, BVI Time-Series Photometry) from Jan 2003 till May 2004 [22] . In these spectra only late-type absorption features were present and it was inconsistent with the spectra that was obtained by Bond in the discovery paper [22] and Szdoky [23]. Time-resolved BVI photometry of the PSR J1023+0038 illustrated an orbital color modulation consistent with a heating effect suggested by Bond [18]. Obtained mean spectrum was similar to a late-type star with no emission lines and from the flux level, $V = 17.5$ could be inferred. The K- and M-dwarf library spectra were too cold to match the mean spectral type of the companion star. Therefore, G-type library spectra from Jacoby et al. (1984) was used to match with mean spectral type and it was accomplished around mid-G admissibly. In consistency with the spectral type the companion's $T_{eff.0}$ was defined in a narrow range between 5570 and 5740 K due to their model [22]. Due to the fact that the distance can be derived by knowing the mass of the companion star, it was expressed as $(2.2 \text{ kpc})(M_2 / M_\odot)^{\frac{1}{3}}$ [22] . Inconsistent with Bond et al. (2002) [18], they offered that the primary is not a white dwarf and only two possibilities remain: a neutron star or a black hole. The strong $\lambda 4686$ line in the Bond et al (2002) high-state spectrum is consistent with an X-ray binary but, unfortunately, no X-ray sources were detected at that time. Shortage of X-ray sources as a primary star can be explained through observation of the source in its quiescence phase as they suggested [22]. In the case of black hole as a primary star, it is not reasonable to have a compact object that has the luminosity of $\sim 2\, L_\odot$ without forming any emission lines, as they mentioned [22].

Patruno and his colleagues used Swift UVOT/XRT telescopes on 2013 June and October for the first targeted X-ray and optical observations of PSR J1023+0038 in its active phase (LMXB) [24]. Images exhibited obvious state change in both UV and optical emissions that were related to the state change of the PSR J1023+0038 [24]. The magnitude of the source was 3.5 higher on 18 Oct with the comparison to 12 June in the UW1 (2600 A) filter. In addition, the magnitude increased and reached 16.04 ± 0.03 in the U band (3465 A). Further observation in U band on 19 Oct illustrated the variability of ~ 0.3 magnitude on a timescale of ~ 1 hour and there was no correlation between the mean 0.5 - 10 keV X-ray luminosity and the U band magnitude. This behavior of U band variability verified the existence of accretion disk

in the binary system.

PSR J1023+0038 was fitted into the X-ray/optical diagram [25, 26] by [24] and supported the concept of relating the observed X-ray and optical luminosity to the accretion process more than to the intrabinary shock or to the spin-down luminosity of the rotation-powered pulsar.

3. OBSERVATION AND DATA REDUCTION

3.1 Optical Observations

3.1.1 T60 Telescope

We used Turkish National Observatory (TUG) T60 robotic telescope[1] which is located in Bakırlıtepe, Antalya through the "Observations to Detect the Low Mass X-ray Binaries Discontinuous Bursts in any wavelength" project (project number 13AT60-433 and 13AT60-613)[2]. The optical classification of the telescope is Ritchey-Chretien. Ritchey-Chretien telescopes are reflecting type of telescopes with parabolic mirrors as shown in Figure 3.1.Switching the spherical main and secondary mirrors with parabolic mirrors have the advantages of eliminating the spherical aberration and decreasing the coma aberration. T60 has a mirror diameter of 60 cm and focal length of 600 cm. In its focal plane it is equipped with a Charge Coupled Device (CCD)[3] with 2048×2048 pixels. The size of the pixels are 15×15 micron and readout time for 2048×2048 pixels is 2.5 sn. The CCD is equipped with different filters, such as Bessell UBVRI (ultraviolet, blue, visible, red and infrared), SDSS and ND. We used the Bessell UBVRI filter and got images in blue, red and infrared.

[1] http://www.tug.tubitak.gov.tr/t60_ozellikler.php

[2] "Galaktik Süreksiz Düşük Kütleli X-ışın Çiftlerinin Herhangi bir Dalgaboyunda Tespit edilecek Patlamalarının Takip Gözlemleri"

[3] http://www.tug.tubitak.gov.tr/t60_fli_ccd.php

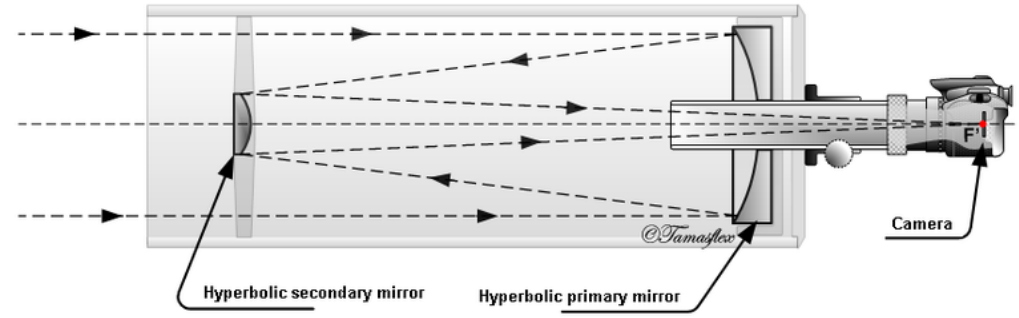

Figure 3.1 : Structure of Ritchey-Chretien Telescope [27].

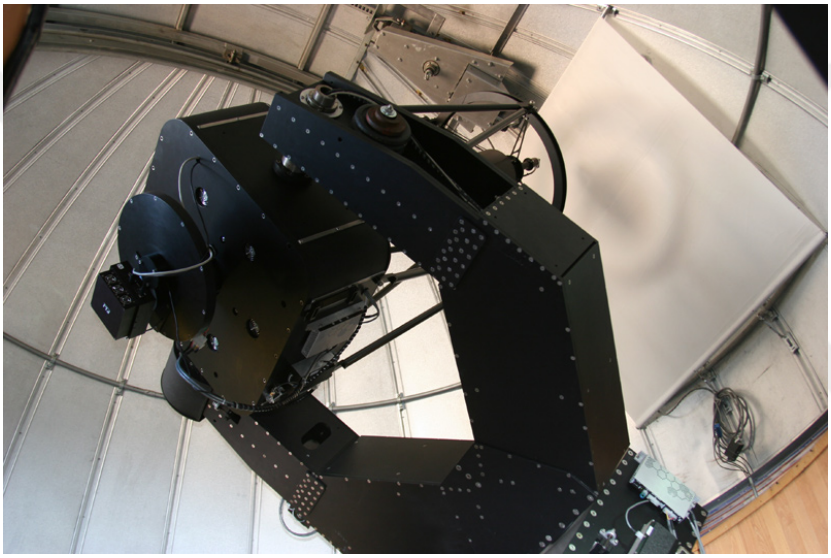

Figure 3.2 : T60 telescope of TÜBiTAK Observatory [28].

Figure 3.3 : Image of FLI CCD [29].

3.2 Optical Data Reduction

Data collected from detectors should be processed for further investigations. In this section, the processing procedure is discussed in detail.

Data processing of optical observations is divided into two parts, data reduction, and data calibration. Optical data reduction has been done by `IRAF` program (Image Reduction and Analysis Facility) [30] and Python is used in the case of data calibration. Before any process was done, we have to pick proper optical frames. Unfortunately we have lost most of the frames due to bad weather condition. We used 74 frames among total 226 frames with 60 second exposure in the red band.

Data reduction contains three steps, dark correction, bias correction and flat correction. In general, final data is obtained as:

$$Final\ data = \frac{(row\ data\ frame - bias\ frame) - (dark\ frame - bias\ frame)}{flat\ frame - dark\ frame} \quad \textbf{(3.1)}$$

Dark correction is needed since the CCD produce some current just because of thermal agitation. Dark frames are provided by exposing the CCD in a condition that no light beams hit the detector and recording the random CCD dark currents. The exposure time of dark frames should be same as the exposure time of frames that will be corrected with these dark frames. In addition to dark current, detectors show some signals in closed shutter and zero exposure time condition, mostly due to the electrical part of the detecting system. These signals are called bias and in some cases, it should be subtracted from data frames (since the dark frames even suffer from bias, subtraction of dark frames is enough in most of the reduction process). Another vital correction is flat field correction. This instrumental noise occurs due to the difference in quantum efficiency of the detector‘s cell and optical transmission over the field of observation. Briefly, detector‘s cells register different amounts of signal for a uniform incident photon flow. Different techniques are available to make flat frames and overcome this problem. Flat frames are produced by exposing a white curtain inside the observatory dome (dome flat) or aiming the telescope to a clear sky condition in daylight (sky flat). As flat frames suffer from the dark current too, dark correction should be applied for both flat and data frames. Two kinds of dark frames were available in 1 second and 60 second. Since for dark reduction of flat and data frames we need equally exposed

dark frames according to each flat and data frames, 1 second dark frames were used to produce 15 seconds dark frames through `imarith` package of `IRAF` for flat frames with 15 seconds exposure and 60 seconds dark frames directly was applied for data frames.

The procedure of reduction began by subtracting the dark frames from flat frames, then followed by subtracting the darks from data frames. At the end, data frames divided by the dark reduced flat frames through CCDPROC package of IRAF. Standard aperture photometry was done on the frames and differential magnitude method was exploited to reduce the error of the analyze. We use 5 nearby stars to compare with the target (PSR J1023+0038). Figure 3.4 illustrates the target and comparison stars, in addition Table 3.1 shows the details of the target and comparison stars that were used in the analysis.

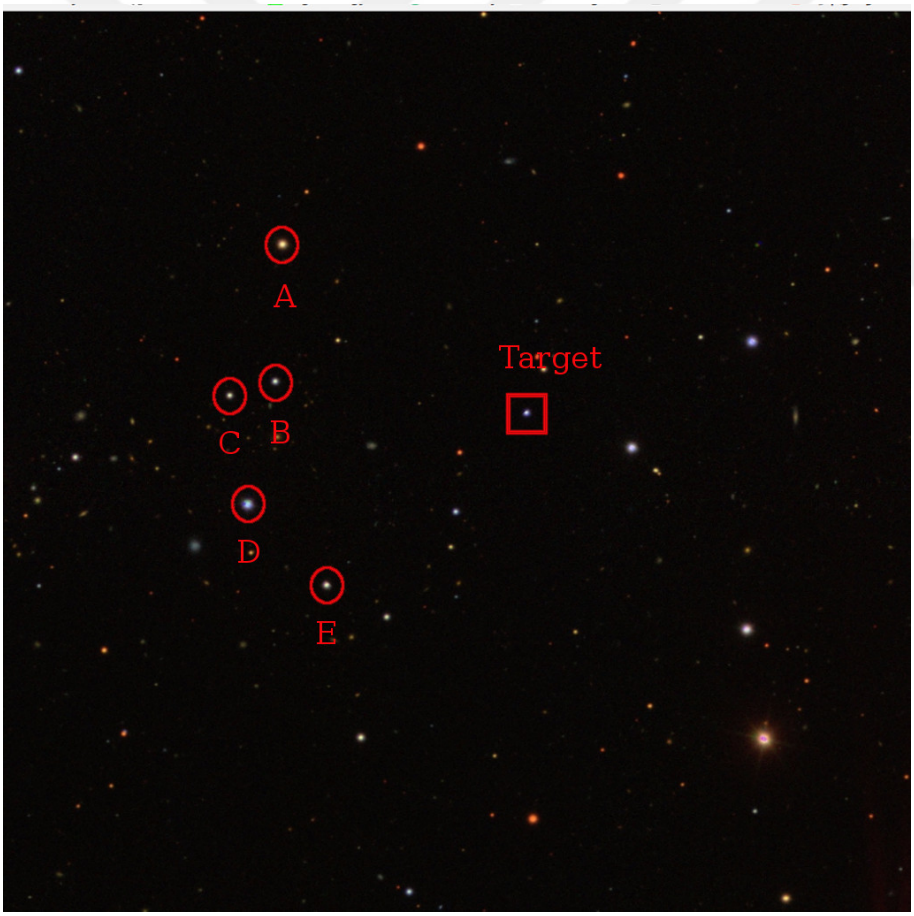

Figure 3.4 : PSR J1023+0038 and comparison stars.

Table 3.1 : Target and comparison stars.

	RAJ2000	DECJ2000	B1 Magnitude	R1 Magnitude	B2 Magnitude	R2 Magnitude
Target star	10 23 47.687	+00 38 41.15	17.59	16.79	17.33	16.96
Star A	10 23 57.990	+00 40 27.70	16.67	15.03	16.45	14.99
Star B	10 23 58.339	+00 39 00.89	17.54	16.26	17.06	16.26
Star C	10 24 00.233	+00 38 52.15	18.01	16.63	17.71	16.52
Star D	10 23 59.435	+00 37 43.26	15.06	14.75	15.35	14.54
Star E	10 23 56.131	+00 36 52.01	17.43	16.13	17.00	16.01

To control the error of differential photometry we calculate the weighted mean of the magnitude of comparison stars according to their magnitude error given by `iraf`. Then the light curve of the PSR J1023+0038 was produced as shown in Figure 3.5. Figure 3.6 shows the light curve of comparison stars at the same time and date of observation of PSR J1023+0038.

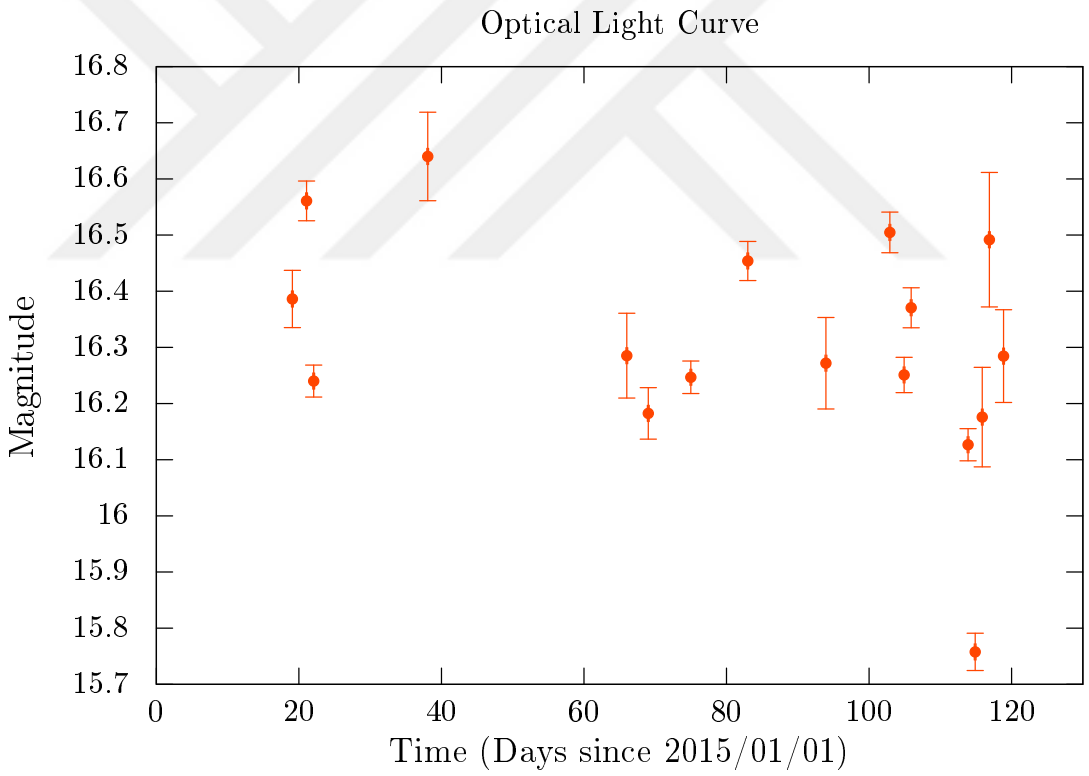

Figure 3.5 : Light curve of PSR J1023+0038 obtained with TÜBiTAK T60 telescope.

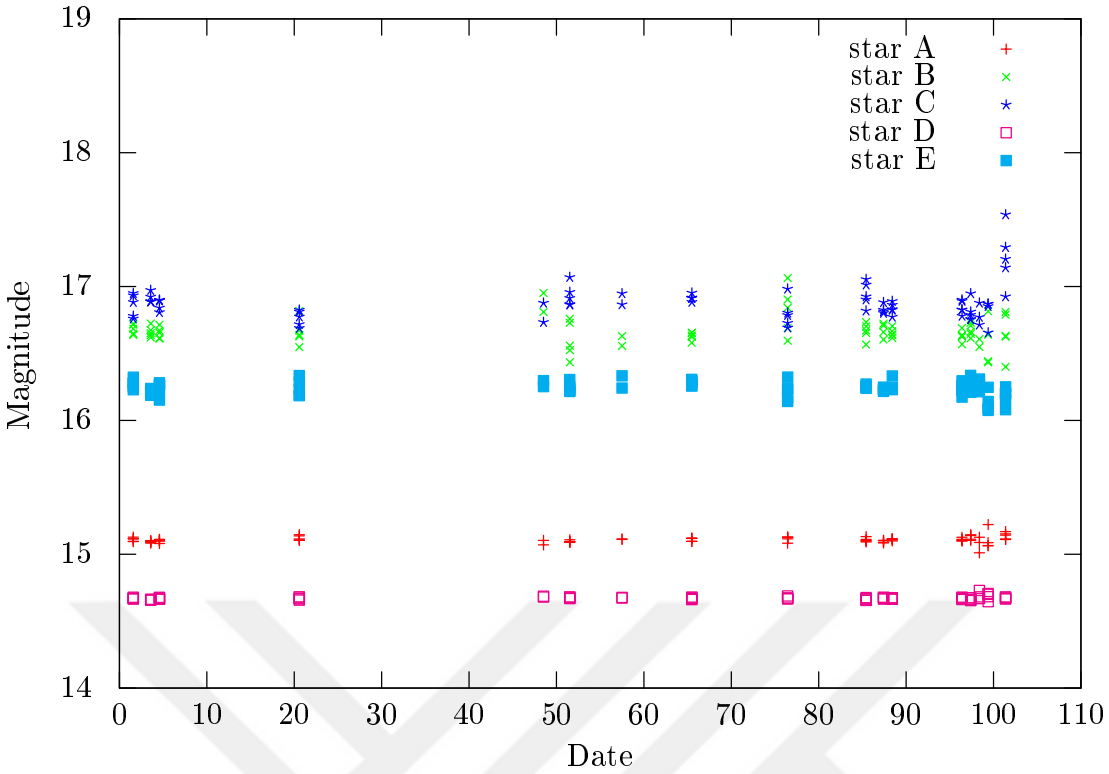

Figure 3.6 : Light curves of comparison stars.

3.3 X-ray Observations

3.3.1 Swift Satellite

The Swift X-ray mission is a project dedicated to studying Gamma-Ray Bursts (GRBs) and their afterglows. It was launched in November of 2004 and settled in a low-earth orbit ($r \sim 160 - 2000$ km). The Swift is equipped with three different telescopes: a Burst Alert Telescope (BAT), an Ultraviolet/Optical Telescope (UVOT) and an X-ray telescope (XRT). The Swift XRT has the ability to evaluate spectra, fluxes, and light curves of the sources.

The **BAT** is designed to detect gamma-ray bursts and other gamma-ray transients in the energy ranges of $15-150$ keV. It has a wide field of view of around 1.4 steradians and can calculate the position of bursts with an accuracy of 1-3 arcminutes.

The **UVOT** is 30 cm ultraviolet/optical telescope with the focal ratio of 12.75 which has modified Ritchey-Chretien structure. It is functional between 1600 Å$-$6000 Å wavelengths and has the ability to locate the bursts positions with an accuracy 0.5 arcseconds.

The **XRT** is a focusing X-ray telescope that has a narrow field of view. Different components of the XRT are shown in Figure 3.8 and the basic parameters are listed in Table 3.2. It is designed to do both imaging and spectroscopy in the energy band between 0.2 and 10 keV. The XRT works in four different mode: imaging mode, photodiode mode, windowed timing mode and photon-counting mode.

The photodiode mode is used in the case of very bright sources (fluxes up to 60 Crab) and when high time resolution is needed. This mode has a time resolution of 0.14 milliseconds and, the ability to produce spectrum and high resolution lightcurve. No spatial data is available in this mode.

In the window timing mode 200 central column, equal to 8 arc second, and 600 row of the CCD is read out during the observation. This mode has the ability to do the observations in 1.7 ms time resolution and is suitable for sources with fluxes between $1-600$ mCrab.

Observation in photon counting mode provides the full field of view but constrains the time resolution to 2.5 seconds as full spectroscopic and imaging resolution is provided in this mode. This mode can be used for sources with fluxes below 1 mCrab.

In imaging mode, there is no distinction of any X-ray event and the CCD completely works same as optical CCD. The XRT uses this mode to determine the position of the new detected GRB accurately. No spectroscopic data is available in this mode due to pile-up in the CCD but the flux of the source can be evaluated acceptably. This mode can be used for the source fluxes between 25 mCrab and 45 Crab [31] and due to the sources flux, the time resolution can be adjusted to 0.1 or 2.5 seconds.

Table 3.2 : XRT characteristics [32]

Telescope	3.5m Wolter I
Telescope PSF	18 arcsec HDP @ 1.5 keV 22 arcsec HDP @ 8.1 keV
Detector	MAT CCD-22
Detector Format	600×602 pixels
Detector Readout Mode	Photon-counting, Imaging & Timing
Field of View	23.6×23.6 arcmin
Pixel Scale	2.36 arcsec/ pixel
Energy Range	0.2 - 10 keV
Effective Area	135 cm^2 @ 1.5 keV
Sensitivity	2×10^{-14}ergs/cm^2/s in10^4s
Position Accuracy	2.5 arcseconds
Operation	Autonomous

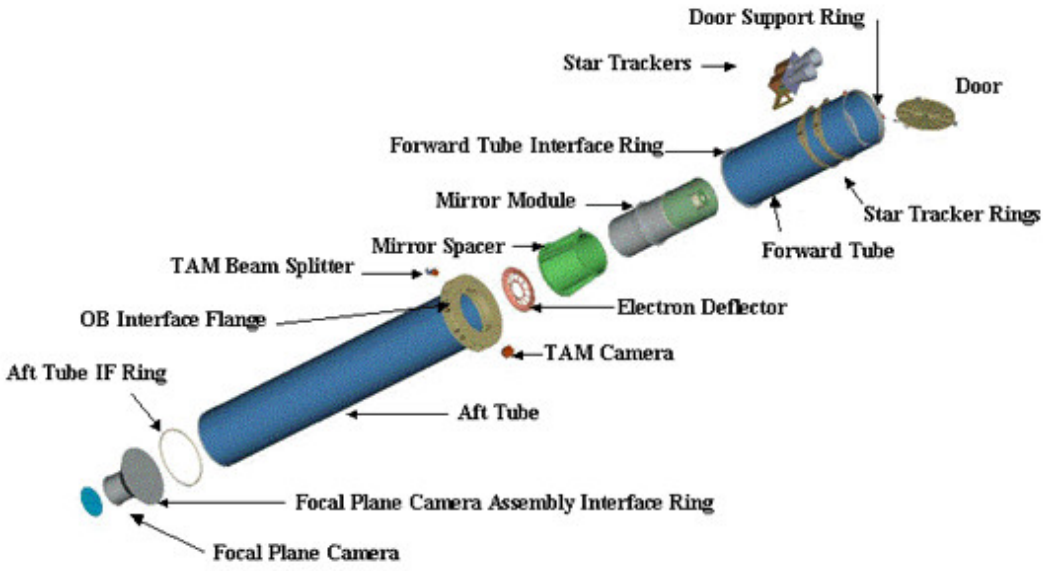

Figure 3.7 : XRT telescope components.

3.3.2 X-Ray Data Analysis

Since we plan to check the properties of the PSR J1023 in both optical and X-ray bands, X-ray data have chosen in a time interval that cover the optical observations time. In total, twenty Swift XRT telescope observations lie between January 01 and 30 April of 2015. Figure 3.8 shows time spanning of both optical and X-ray observations. Appendix A.1 contains observation IDs (Obs ID) that is used for the analysis. We used number of `FTOOLS`[4] from the `Heasoft v 6.19`[5] packages through the X-ray analysis.Swift level 2 data (event file) and ancillary file for each Obs ID extracted by applying `xrtpipeline` on level 1 data. For the response matrix, `swxpc0to12s6-20130101v014.rmf` file from Caldb is used for all Obs IDs. Source and background regions have been determined as circular region with 40 arcsecond radius manually via the `Ds9` program for individual Obs IDs (Figure 3.9). Source and background spectrums and light curves extracted using `xselect`. To achieve reasonable data and applying models, `XSPEC` was used. First data grouped fot 20 count/s via `grppha`, then extra calibration applied to data as explained here, bad channels were removed through `XSPEC` and the data was fitted with absorbed powerlaw model. N_H was fixed to 3.8×10^{20} cm^{-2} [24]. We obtained mean photon index as $\Gamma \simeq 1.5$. Figure 3.11. to Figure 3.13. show the spectrum and model fitted

[4] `https://heasarc.gsfc.nasa.gov/ftools/ftools_menu.html`
[5] `https://heasarc.nasa.gov/lheasoft/`

with residuals. Photon index and X-ray luminosity that were obtained by applying the absorbed powerlaw model on the data is illustrated in Figure 3.14 and Figure 3.15, respectively.

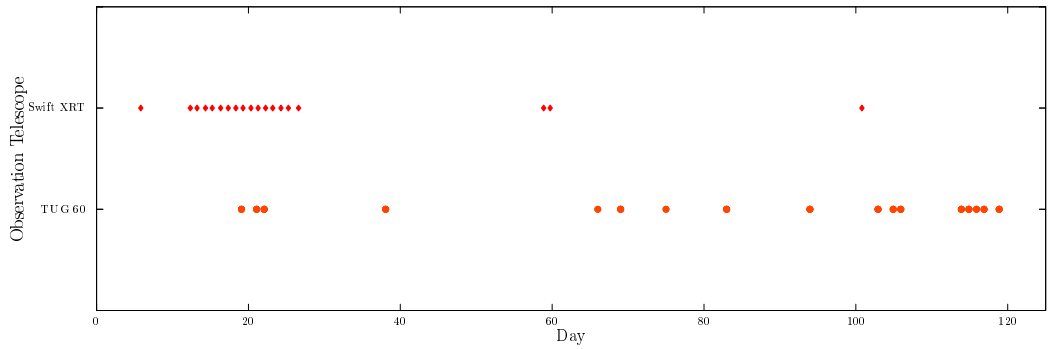

Figure 3.8 : Time spans of optical and X-ray observations.

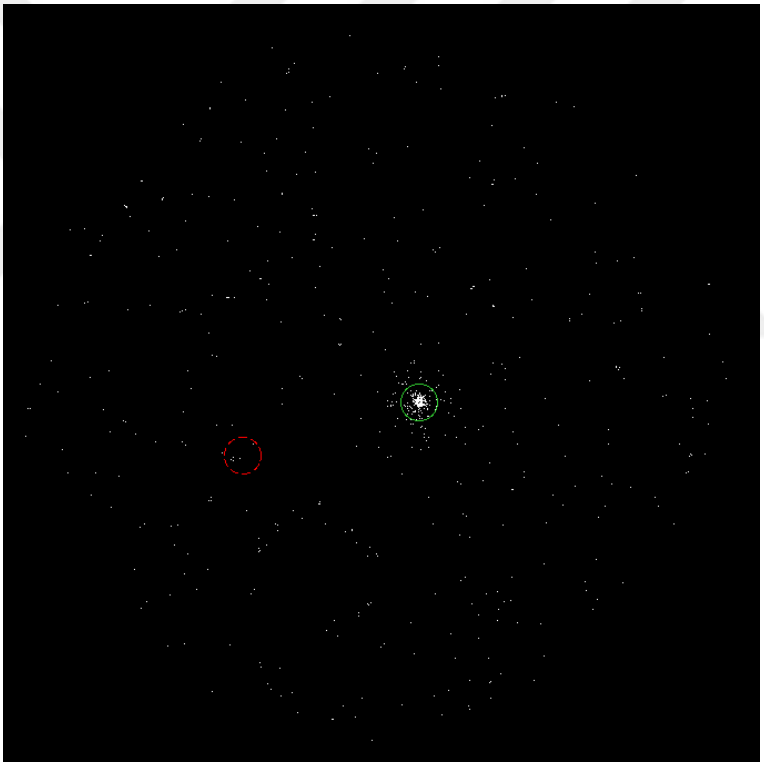

Figure 3.9 : An example of source (green) & background (red dashed circle) region selection.

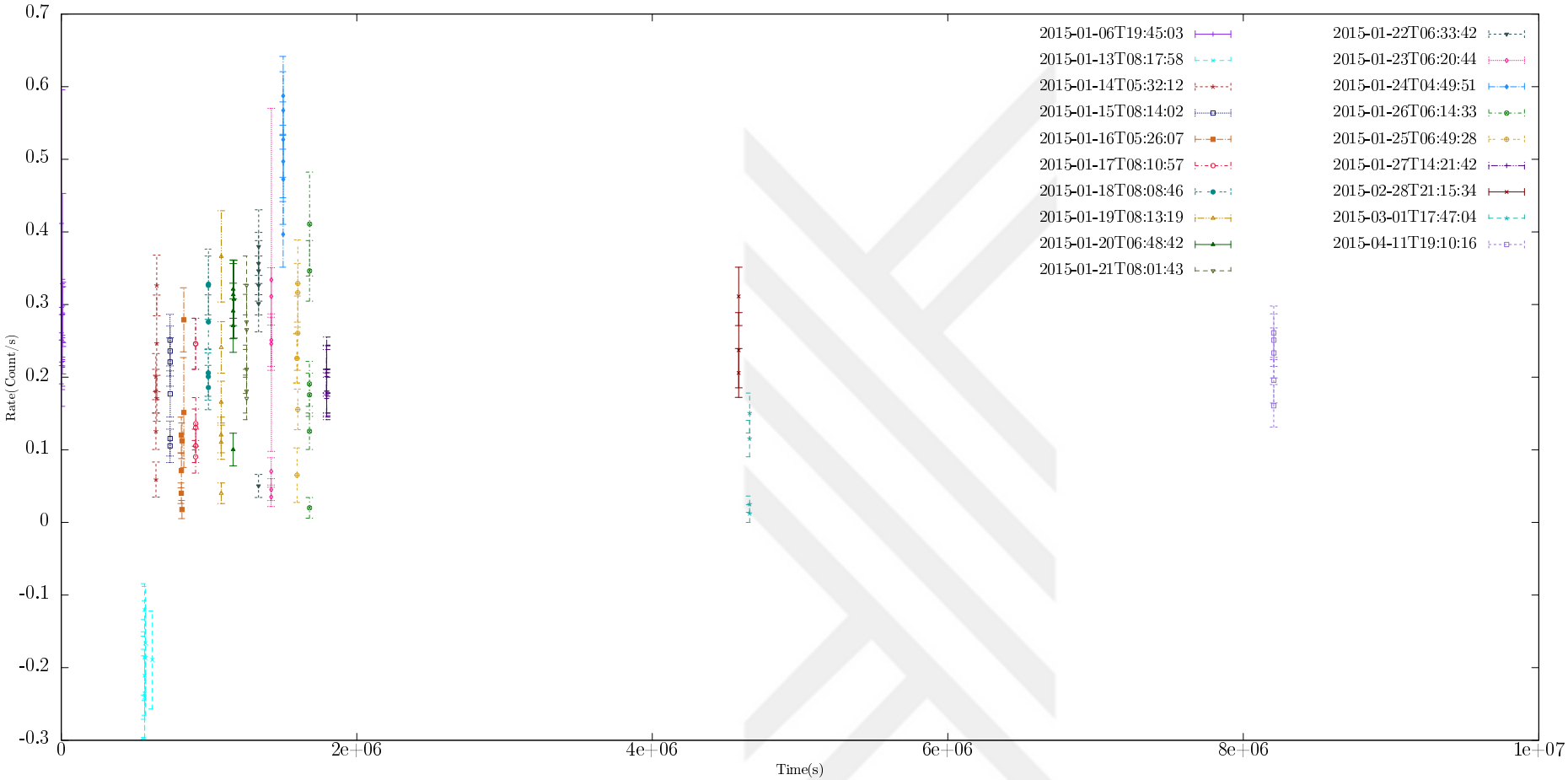

Figure 3.10 : X-ray observation light curves.

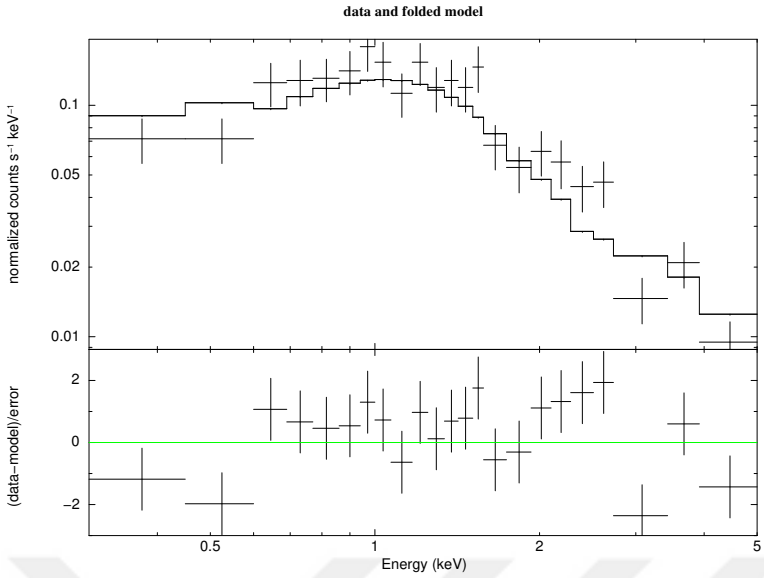

Figure 3.11 : Spectrum fitted with absorbed powerlaw.

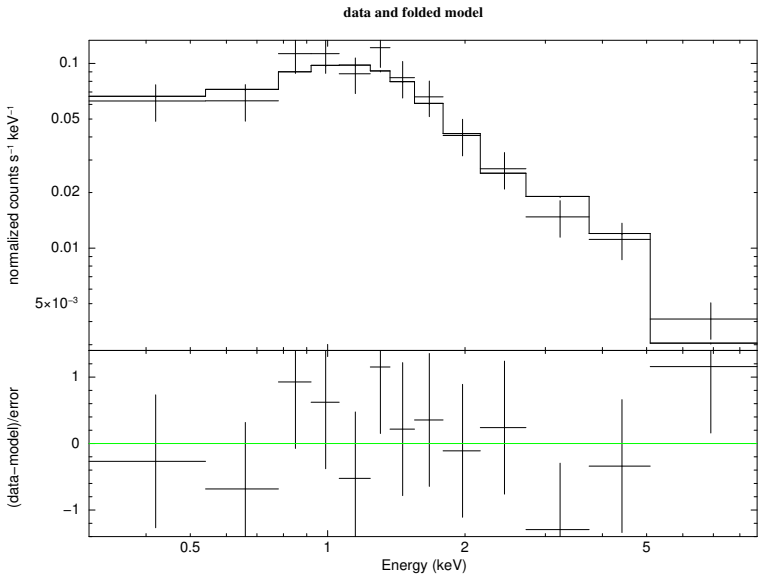

Figure 3.12 : Spectrum fitted with absorbed powerlaw.

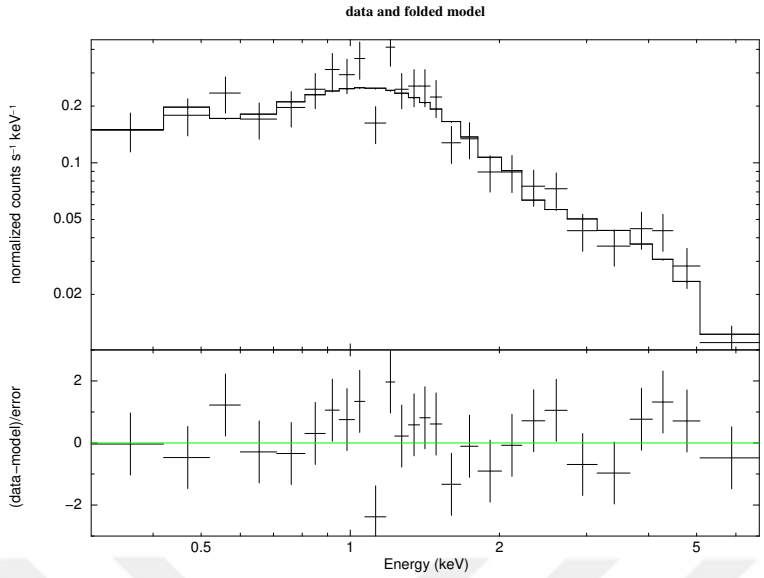

Figure 3.13 : Spectrum fitted with absorbed powerlaw.

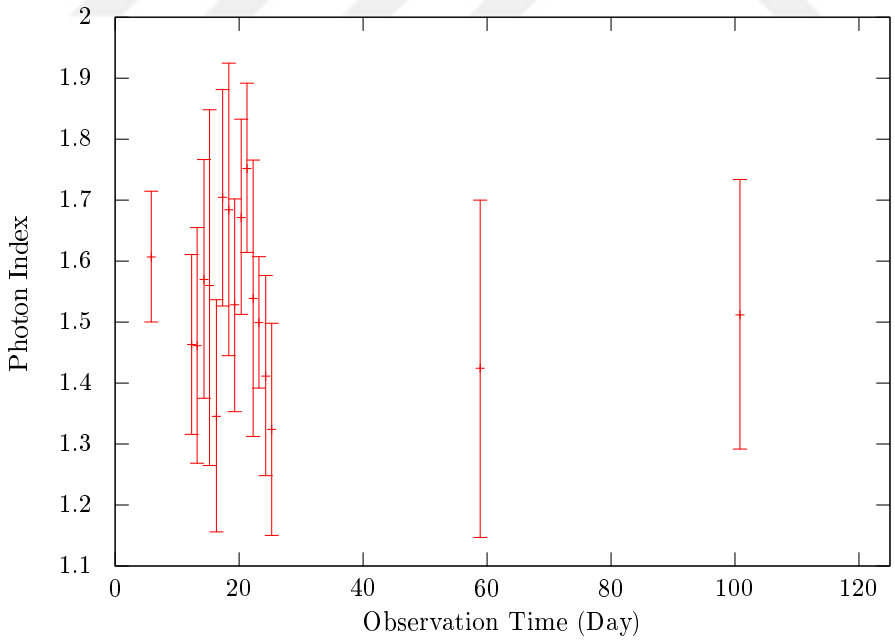

Figure 3.14 : Photon index of PSR J1023+0038.

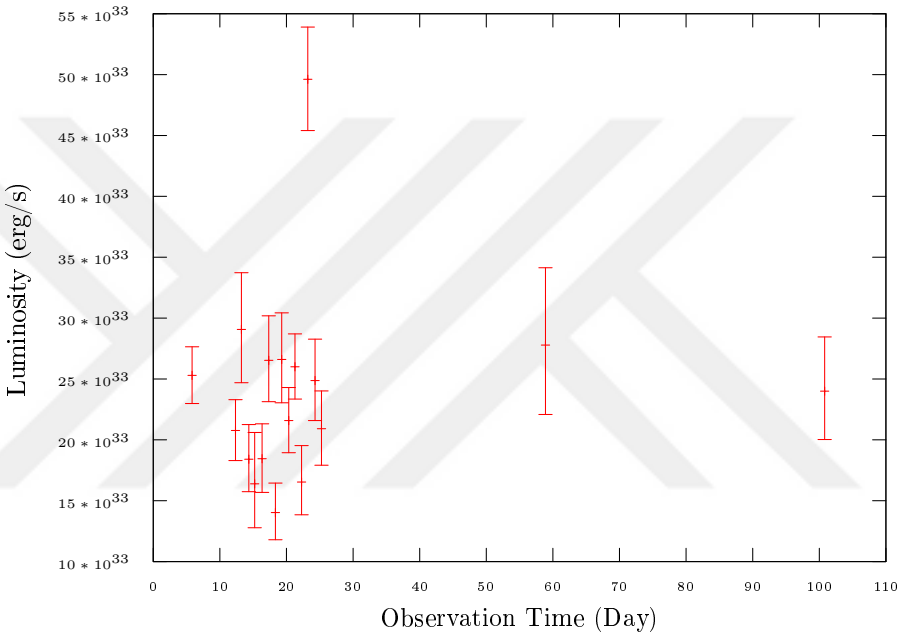

Figure 3.15 : X-ray luminosity of PSR J1023+0038.

4. CONCLUSION

We obtained optical luminosity between 15.57 and 16.95 in r band (mean 16.31). Magnitude variation of $\sim$ 1.38 in r band could be the result of orbital rotation of the system with 4.7 hour orbital period. Low time resolution of the data does not let us to check for any uniform variation in optical magnitude due to orbital rotation of the system. On the other hand poor seeing condition during the optical observations decrease the reliability of the measurements.

In the case of X-ray luminosity, we obtained 1.4×10^{33} erg/s $\lesssim L_X \lesssim$ 4.9×10^{33} erg/s that shows the system was in LMXB phase with low X-ray flux.

In general correlation between X-ray and optical luminosity in LMXB systems is expected. Many different mechanisms can lead to increase in optical luminosity. Reprocessing from an irradiated disk is one of the mechanisim that was suggested by [33]. We investigate to find optical-X-ray correlation in TMP, PSR J1023+0038. As it was shown in Figure 3.8 our data suffers the lack of simultaneous observation in optical and X-ray wavelength and we are unable to put trustable comment on existence or non existence of the correlation in PSR J1023+0038.

REFERENCES

[1] **Hewish, A.**, **Bell, S.J.**, **Pilkington, J.D.H.**, **Scott, P.F. and Collins, R.A.** (1968). Observation of a Rapidly Pulsating Radio Source, *Nature*, ***217***, 709–713.

[2] **Gold, T.** (1968). Rotating Neutron Stars as the Origin of the Pulsating Radio Sources, *Nature*, ***218***, 731–732.

[3] **Url-1**, `https://public.nrao.edu/radio-astronomy/pulsars/`.

[4] **Manchester, R.N.**, **Hobbs, G.B.**, **Teoh, A. and Hobbs, M.** (2005). The Australia Telescope National Facility Pulsar Catalogue, *AJ*, ***129***, 1993–2006, `astro-ph/0412641`.

[5] **Alpar, M.A.**, **Cheng, A.F.**, **Ruderman, M.A. and Shaham, J.** (1982). A new class of radio pulsars, *Nature*, ***300***, 728–730.

[6] **Zel'dovich, Y.B. and Shakura, N.I.** (1969). X-Ray Emission Accompanying the Accretion of Gas by a Neutron Star, *Soviet Astronomy*, ***13***, 175.

[7] **Davidson, K. and Ostriker, J.P.** (1973). Neutron-Star Accretion in a Stellar Wind: Model for a Pulsed X-Ray Source, *ApJ*, ***179***, 585–598.

[8] **Lamb, F.K.**, **Pethick, C.J. and Pines, D.** (1973). A Model for Compact X-Ray Sources: Accretion by Rotating Magnetic Stars, *ApJ*, ***184***, 271–290.

[9] **den Heuvel, V.** (2001). *Formation and Evolution of Neutron Star Binaries*, Cambridge University Press.

[10] **F., V.** (1995). *X-ray Binaries*, Cambridge University Press.

[11] **Gosh, P.** (2007). *Rotation and Accretion Powered Pulsars*, World Scientific Publishing Co.

[12] **Hulse, R.A. and Taylor, J.H.** (1975). Discovery of a pulsar in a binary system, *ApJ*, ***195***, L51–L53.

[13] **Bisnovatyi-Kogan, G.S. and Komberg, B.V.** (1974). Pulsars and close binary systems, *Soviet Astronomy*, ***18***, 217.

[14] **Bisnovatyi-Kogan, G.S. and Komberg, B.V.** (1976). Possible evolution of a binary-system radio pulsar as an old object with a weak magnetic field, *Soviet Astronomy Letters*, ***2***, 130–132.

[15] **Backer, D.C.**, **Kulkarni, S.R.**, **Heiles, C.**, **Davis, M.M. and Goss, W.M.** (1982). A millisecond pulsar, *Nature*, ***300***, 615–618.

[16] **Radhakrishnan, V. and Srinivasan, G.** (1982). On the origin of the recently discovered ultra-rapid pulsar, *Current Science*, ***51***, 1096–1099.

[17] **Wijnands, R. and van der Klis, M.** (1998). A millisecond pulsar in an X-ray binary system, *Nature*, ***394***, 344–346.

[18] **Bond, H.E.**, **White, R.L.**, **Becker, R.H. and O'Brien, M.S.** (2002). FIRST J102347.6+003841: The First Radio-selected Cataclysmic Variable, *Publications of the Astronomical Society of the Pacific*, ***114***, 1359–1363, astro-ph/0208383.

[19] **Gregg, M.D.**, **Becker, R.H.**, **White, R.L.**, **Helfand, D.J.**, **McMahon, R.G. and Hook, I.M.** (1996). The First Bright QSO Survey, *AJ*, ***112***, 407, astro-ph/9604148.

[20] **White, R.L.**, **Becker, R.H.**, **Gregg, M.D.**, **Laurent-Muehleisen, S.A.**, **Brotherton, M.S.**, **Impey, C.D.**, **Petry, C.E.**, **Foltz, C.B.**, **Chaffee, F.H.**, **Richards, G.T.**, **Oegerle, W.R.**, **Helfand, D.J.**, **McMahon, R.G. and Cabanela, J.E.** (2000). The FIRST Bright Quasar Survey. II. 60 Nights and 1200 Spectra Later, *ApJS*, ***126***, 133–207, astro-ph/9912215.

[21] **Becker, R.H.**, **White, R.L.**, **Gregg, M.D.**, **Laurent-Muehleisen, S.A.**, **Brotherton, M.S.**, **Impey, C.D.**, **Chaffee, F.H.**, **Richards, G.T.**, **Helfand, D.J.**, **Lacy, M.**, **Courbin, F. and Proctor, D.D.** (2001). The FIRST Bright Quasar Survey. III. The South Galactic Cap, *ApJS*, ***135***, 227–262, astro-ph/0104279.

[22] **Thorstensen, J.R. and Armstrong, E.** (2005). Is FIRST J102347.6+003841 Really a Cataclysmic Binary?, *AJ*, ***130***, 759–766, astro-ph/0504523.

[23] **Szkody, P.**, **Fraser, O.**, **Silvestri, N.**, **Henden, A.**, **Anderson, S.F.**, **Frith, J.**, **Lawton, B.**, **Owens, E.**, **Raymond, S.**, **Schmidt, G.**, **Wolfe, M.**, **Bochanski, J.**, **Covey, K.**, **Harris, H.**, **Hawley, S.**, **Knapp, G.R.**, **Margon, B.**, **Voges, W.**, **Walkowicz, L.**, **Brinkmann, J. and Lamb, D.Q.** (2003). Cataclysmic Variables from the Sloan Digital Sky Survey. II. The Second Year, *AJ*, ***126***, 1499–1514, astro-ph/0306269.

[24] **Patruno, A.**, **Archibald, A.M.**, **Hessels, J.W.T.**, **Bogdanov, S.**, **Stappers, B.W.**, **Bassa, C.G.**, **Janssen, G.H.**, **Kaspi, V.M.**, **Tendulkar, S. and Lyne, A.G.** (2014). A New Accretion Disk around the Missing Link Binary System PSR J1023+0038, *ApJ*, ***781***, L3, 1310.7549.

[25] **Russell, D.M.**, **Fender, R.P.**, **Hynes, R.I.**, **Brocksopp, C.**, **Homan, J.**, **Jonker, P.G. and Buxton, M.M.** (2006). Global optical/infrared-X-ray correlations in X-ray binaries: quantifying disc and jet contributions, *MNRAS*, ***371***, 1334–1350, astro-ph/0606721.

[26] **Russell, D.M.**, **Fender, R.P. and Jonker, P.G.** (2007). Evidence for a jet contribution to the optical/infrared light of neutron star X-ray binaries, *MNRAS*, ***379***, 1108–1116, 0705.3611.

[27] **Url-4**, https://commons.wikimedia.org/wiki/File:Ritchey-ChrC3A9tien.jpg.

[28] **Url-2**, http://www.tug.tubitak.gov.tr/images/t60/t60_1.jpg.

[29] **Url-3**, http://www.flicamera.com/proline/images/ProLine3.jpg.

[30] **Tody, D.** (1993). IRAF in the Nineties, ***R.J. Hanisch**, **R.J.V. Brissenden and J. Barnes**, editors, Astronomical Data Analysis Software and Systems II*, volume 52 of *Astronomical Society of the Pacific Conference Series*, p.173.

[31] **Capalbi, M.**, **Perri, M.**, **Saija, B. and Tamburelli, F.** (2005). The Swift XRT Data Reduction Guide.

[32] **Burrows, D.N.**, **Hill, J.E.**, **Nousek, J.A.**, **Kennea, J.A.**, **Wells, A.**, **Osborne, J.P.**, **Abbey, A.F.**, **Beardmore, A.**, **Mukerjee, K.**, **Short, A.D.T.**, **Chincarini, G.**, **Campana, S.**, **Citterio, O.**, **Moretti, A.**, **Pagani, C.**, **Tagliaferri, G.**, **Giommi, P.**, **Capalbi, M.**, **Tamburelli, F.**, **Angelini, L.**, **Cusumano, G.**, **Bräuninger, H.W.**, **Burkert, W. and Hartner, G.D.** (2005). The Swift X-Ray Telescope, *Space Science Reviews*, ***120***, 165–195, astro-ph/0508071.

[33] **Bernardini, F.**, **Cackett, E.M.**, **Brown, E.F.**, **D'Angelo, C.**, **Degenaar, N.**, **Miller, J.M.**, **Reynolds, M. and Wijnands, R.** (2013). Daily multiwavelength Swift monitoring of the neutron star low-mass X-ray binary Cen X-4: evidence for accretion and reprocessing during quiescence, *MNRAS*, ***436***, 2465–2483, 1307.2492.

APPENDICES

APPENDIX A.1 : Observation IDs of Swift XRT telescope.

APPENDIX A:

Table A.1 : Swift X-Ray Observation of PSR J1023+0038 .

Obs ID	Date	Time	Exp. Time
00033012068	2015-01-06	19:45:03	$1.942891084038568E+03$
00033012070	2015-01-13	08:17:58	$1.323579889157465E+03$
00033012071	2015-01-14	05:32:12	$1.153755670881827E+03$
00033012072	2015-01-15	08:14:02	$1.176221083455461E+03$
00033012073	2015-01-16	05:26:07	$9.989349134039215E+02$
00033012074	2015-01-17	08:10:57	$1.113789566374350E+03$
00033012075	2015-01-18	08:08:46	$1.126275794266340E+03$
00033012076	2015-01-19	08:13:19	$1.093811343670687E+03$
00033012077	2015-01-20	06:48:42	$1.076340453057892E+03$
00033012078	2015-01-21	08:01:43	$1.063844164203505E+03$
00033012079	2015-01-22	06:33:42	$1.146254147496361E+03$
00033012080	2015-01-23	06:20:44	$1.191204720235088E+03$
00033012081	2015-01-24	04:49:51	$1.118784138399841E+03$
00033012082	2015-01-26	06:14:33	$1.076330533680910E+03$
00033012083	2015-01-25	06:49:28	$1.036384243178606E+03$
00033012084	2015-01-27	14:21:42	$1.665684793487728E+03$
00033012085	2015-02-28	21:15:34	$4.769869967561585E+02$
00033012086	2015-03-01	17:47:04	$7.666697913576909E+02$
00033012088	2015-04-11	19:10:16	$9.914236785218692E+02$

CURRICULUM VITAE

Name Surname: Hesaum Farazi Majd

Place and Date of Birth: Tehran/Iran 07/04/1984

Adress: Technical University of İstanbul, Faculty of Art and Science, Department of Physics Engineering, L1-303, 34469, Maslak İstanbul

E-Mail:farazimajdh@itu.edu.tr ; hfm.physics@gmail.com

B.Sc.: Department of Applied Physics, Tabriz Azad University